The Effect of Input Pulse on the Soliton Generation in Microresonators

Hawraa A. Mezban *[1a] and H. A. Sultan [1b]

[1] Department of Physics ,College of Education for Pure Sciences, University of Basrah, Basrah, Iraq.

[b]E-mail: hassabd67@yahoo.com
[a*]Corresponding author: hawraaalhassen@gmail.com

Abstract—The effect of the input pulse (chirped pulse) on the generation of soliton wave and optical frequency comb in microresonators was studied. The problem was solved numerically using the Lugiato-Lefever equation and the Fourier method by MATLAB program. The effect of Gaussian and ultra-Gaussian pulses, as well as chirped pulses, on the generation of the soliton wave and the frequency comb was also studied. Our study demonstrated that the generation of the soliton and the frequency comb depends on the shape of the pulse intensity distribution. Moreover, the mobility of the soliton and comb changes depending on the shape of the pulse. In addition, the results showed us that the soliton and frequency comb generated in microresonators are strongly affected by the power of the incoming pulse and the radius of the microresonator.

Keywords—Frequencychirp,Super-gaussian pulse, Lugiato–Lefever equation, solitons, nonlinear optics.

I. INTRODUCTION

Solitary wave dynamic research is very common research in nonlinear sciences, such as mathematics, optics, condensed matter, chemistry, biology, and soliton [1]. A soliton is a wave packet or pulse that moves steadily by maintaining its shape. They were created when nonlinear and dispersive processes in a medium cancel each other. This process does not follow the superposition principle and does not fade away. Long distances can be covered by soliton waves with little energy or structural loss.

Early research on solitons, especially in optical fibers, made conservative assumptions about the medium's loss lessness and the interplay between nonlinearity and diffractive effects. However, it was shown later that if the system was continuously supplied with an external energy source, solitons might also develop in the presence of dissipation [2].

The Kerr effect and dispersion, in general, cause a modification of the optical pulse's dynamics in the time and spectral form to alter during its propagation in a transparent material. In other words, we can say that the Kerr effect refers to the phenomenon in which the refractive index of the material changes in response to the intensity of the pulse passing through the medium. This effect arises from the interaction between the electromagnetic field of light and the electrons in the material. When light intensity is high, the Kerr effect causes a change in the refractive index, which in turn affects the propagation of light through the material. As for dispersion, it refers to the phenomenon in which different components of the optical pulse travel at different speeds through matter. This happens because different wavelengths of light experience different refractive indices in the material. As a result, the shape and duration of the optical pulse can be changed during propagation, leading to temporal and spectral modulations. When an optical pulse propagates through a transparent material, both Kerr effect and scattering can affect its temporal and spectral properties. In some situations, even with extremely large propagated distances, the pulses' temporal and spectral structure can be preserved due to the precise cancellation of Kerr nonlinearity and dispersion effects, except for a constant phase delay per unit of propagation distance [3, 5]. The soliton generation in conventional and photonic crystal fibers was studied briefly [6-9]. Solitons possess highly attractive features for practical implementation beyond controlled environments due to their compacted dimensions and minimal requirements of energy. It was shown that the equilibrium between the cavity losses, cavity gain, group velocity dispersion (GVD), and Kerr nonlinearity can be maintained to create low-noise, coherent, broad-frequency combs in microresonators[4,10].

In the past ten years, nonlinear physics in microresonators, , including breathing solitons [5], soliton crystals [11], Stokes solitons [12], Pockels solitons [13], laser cavity solitons [14], and dark solitons has been discovered [15].

In this study, we investigated the soliton dynamics in a microresonator that was pumped by a CW source in anomalous dispersion regimes and offered a comprehensive analysis of the influence of starting frequency chirp on Gaussian pulse in SiN microresonator at 1550 nm wavelength. Additionally, we explored the implications of converting the laser beam's super-Gaussian shape, into a standard Gaussian profile.

II. THEORY

The lugiato-Lefever equation (LLE) describes how light flows through a high-finesse resonator or medium. It has been demonstrated that there is a high between the theoretical and experimental results in   determining an equilibrium spectrum solution [16]. This enables us to

describe the temporal profile of the field envelope, which moves in the cavity at this pace. To connect the intracavity field at the end of one round trip with the field at the start of the next round trip, boundary conditions that take each round trip's evolution into account are required. Mathematically, this connection was possible by [17].

$$E^{m+1}(0,\tau) = \sqrt{\theta}E_0 + \sqrt{1-\theta}E^{(m)}(L,\tau)e^{i\varphi_0} \qquad (1)$$

Hence, the intracavity field at the start of the $(m + 1)^{th}$ roundtrip is $E^{m+1}(0, \tau)$ at the end of the mth roundtrip. L is the cavity length for the SiN micro-ring resonator.

Where φ_0 gives the linear phase accumulation of the intracavity field for the pump field over a single roundtrip, and θ gives the external coupling coefficient. In the limit of low loss, the intracavity field envelope can be considered to fluctuate somewhat between consecutive round trips. Under these conditions, the externally driven NLSE may be obtained by averaging the previous infinite-dimensional map[18]

$$t_r \frac{\partial E(t,\tau)}{\partial t} = [-(\alpha + i\delta_o) + iL \sum_{k \geq 2} \frac{\beta_k}{k!} \left(i\frac{\partial}{\partial \tau}\right)^k + iL\gamma|E(t,\tau)|^2]E(t,\tau) + \sqrt{\theta}E_{in} \qquad (2)$$

TABLE 1: THE SIMULATION PARAMETERS USED IN THIS WORK ARE THE TYPICAL PARAMETERS FOR A SILICON NITRIDE (SiN) RING RESONATOR [18, 24, 25].

Table Head	Table Column Head		
	Description	*Value Unit*	*Unit*
λ_0	Lasing Wavelength	1.55	μm
n_2	The nonlinear refractive index	2.4×10^{-19}	m²/W
ω_0	the frequency of the optical cw pump	193.5	THz
n_0	the refractive index	1.99	
A_{eff}	the effective model area of the resonator mode	2.5×10^{-12}	m²
Q	Quality factor	1.5×10^6	
Θ	the external coupling coefficient	0.03	
P_{in}	input cw pump power	0.5, 1, 1.5, 2	Watt
Γ	nonlinearity coefficient	1.2	W⁻¹m⁻¹
A	total cavity losses inside the resonator	0.00161	
β_2	dispersion coefficient	-4.7×10^{-26}	s²m⁻¹
L	Cavity length	428.6	μm
t_r	the roundtrip time	14.28	ns
a	radius	100	μm
τ	Fast time	2	ps

E (t,τ) denotes the intracavity field, the roundtrip duration is t_r (t_r=L/C), and the slow time scale for this profile's progression over consecutive roundtrips is denoted by t. Additionally, it is presumed that the field will follow the cavity roundtrip time, E(t + 2,τ) = E(t,τ), and it determines the field's temporal profile in ordinary (fast) time [19]. The following are the meanings of the other variables in the formula: β represents the dispersion coefficient of second order, α = (αᵢ + θ)/2 denotes the total cavity losses, and δ₀ = 2kπ − φ₀≪1 indicates the order of the cavity resonance that is closest to the driving field when the cavity is detuning from the nearest resonance. The coefficient of power transmission, represented by k, and i associated with the dispersion coefficients β_k, and γ, the nonlinear interaction coefficient.

Using the nonlinear Schrodinger equation (NLSE), the LLE is essentially a periodic boundary condition applied to a damped, driven Kerr nonlinear resonator [20]. A slow-varying time envelope is defined, which is significant since it yields a mean-field solution with no field fluctuations over a round trip. This constraint is what sets the LLE apart from the more general Ikeda map [21]. Provides great physical representation for a wide range of systems while making computations simpler. Particularly, simulations built on the LLE formalism have made it possible to describe the production of microcombs in a way that quantitatively correlates with reported experimental results [22] (e.g., in terms of spectral bandwidth), Additionally, theoretical research has improved understanding of unique nonlinear dynamics that Kerr nonlinear microresonators can support [23].

III. RESULTS AND DISCUSSION:

The split-step Fourier method (SSFM) was used to imitate the soliton dynamics within the LLE numerically [20]. The simulation settings that were employed for this study are shown in Table (1).

a) The effect of the chirped pulse:

In the realm of optical transmission systems, there are a lot of practical applications for chirped solitons. Ultrashort pulses, consisting of very brief bursts of light, are used to transmit information over optical fibers. However, these pulses can experience dispersion, which causes the different frequency components of the pulse to spread out over time. This dispersion can degrade the quality of the transmitted signal [26].

Chirp is a sudden shift in the cavity's center of wavelength caused by cavity instability. When a pulse's rising edge and falling edge have slightly differing frequencies, it chirps. Due to the carrier-induced change in the refractive index by pulses that are created at the transmitter end, the intensity modulation results in phase modulation. The cavity linewidth is the primary cause of that alteration [27].

The Kerr effect which relies on the time-dependent pulse intensity, shifts the phase of the optical pulse during its traveling through the material. This results which is so-

called (chirp). It is a temporal variable instantaneous frequency.

In this study, We provided the results of numerical studies of the cavity soliton (CS) dynamics in the presence of chirped laser pulses in this section. Concurrently, the chirped pulses will cause background amplitude and phase modulation. By applying a negative chirp parameter, the CS trapping sites may be moved closer to the pump pulse maximum, and CS can be consistently trapped at the peak with a high enough chirp value. Furthermore, chirped pulses can increase the range of existence for CSs powered by desynchronized chirped pulses. Apart from offering fresh perspectives on the behavior of CSs produced by chirped optical pulses, our work offered a workable solution for controlling the CSs in passive Kerr resonators.

We explored applying a single pulse to the dominating second-order anomalous dispersive Kerr resonator as we can see in Figure (1). Chirping is a term used when a pulse's carrier frequency changes over time. Frequency change and the phase derivative are closely related. There is a parameter called parameter C that controls the linear frequency chirp applied to the pulse.

We noticed that by changing the value of parameter C, chirped pulses can become broader or narrower. However, a broadened pulse is undoubtedly undesirable. The frequency chirp affects the shape of the optical pulse. In the regime of the anomalous dispersion, there exist straightforward connections among the pulse parameters E, T, and P_0, along with the oscillator parameters β (representing the overall delay dispersion coefficient). γ indicates the self-phase modulation coefficient of a nonlinear medium, such as an active crystal, air, optical plate, etc.)[20].

$$T = \sqrt{|\beta|/\gamma P_o} \ , \ E = 2 \ |\beta|/\gamma T \qquad (3)$$

Energy scaling demands pulse stretching, which can only be accomplished by a large dispersion increase. Pulse instability must be prevented by keeping the peak power P_0 below a certain threshold value P_{th}.

$$E = 2\sqrt{|\beta|P_{th}/\gamma} \qquad (4)$$

The presence of the so-called chirp causes a pulse to be stretched, and its peak power to be lowered in the usual dispersion regime [28]. We analyzed the effect of the initial chirp on the Gaussian pulse during its propagation in a microresonator at a wavelength of 1550 nm. The chirped Gaussian pulse, which we used in this study, was provided by [28]:

$$U(0,T) = U_0 exp \left(- \frac{(1+iC)}{2} \frac{T^2}{T_0^2} \right) \qquad (5)$$

The chirp parameter C describes the frequency variation within the pulse envelope. The Lugatio-Lefever equation must be solved to obtain a thorough description of all impacts on the propagating signal. We built our modeling using femtosecond pulse propagation as was mentioned in [6-9]

The group velocity dispersion (GVD) effect is integrated into the microresonator through a variable represented by β_2. Because the refractive index is affected by the intensity, it created nonlinearity and induced nonlinear chirp in the pulse [29]. The main nonlinear effect is self-phase modulation [30].

During the optical pulse transmission inside an optical fiber, the GVD broadens them. These pulses might be chirped at the beginning or throughout propagation. Specifically, depending on the signs of the chirp parameter C and the GVD parameter β_2, a chirped pulse can be created during the early stages of propagation. The requirement β_2 at C< 0 met since β_2<0 in the 1.55 m wavelength area of silica fibers.

Known as an up chirp or positive chirp, the instantaneous frequency increases linearly from the leading to the trailing edge when C > 0. A down chirp, also known as a negative chirp, is the frequency that falls linearly from the leading to the edge that follows,C< 0. If we set C = 0, this equation will decrease to an unchirped Gaussian pulse as described by Eq. (6), as shown in fig. (3). Due to the combined effects of loss, dispersion, and nonlinearity in both anomalous dispersion regimes.

$$U(0,T) = exp \left(- \frac{T^2}{2T_0^2} \right) \qquad (6)$$

Generally speaking, the chirp was classified as a positive or negative chirp according to whether C is positive or negative.
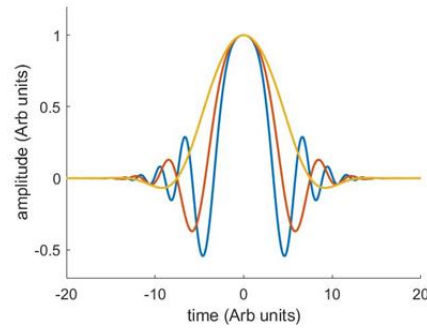

Fig. 1: chirped pulses used as input pulses in the study.

In this study, we used the chirped Gaussian pulse indicated before as input and used the split-step Fourier technique to numerically solve the LLE. This showed that the soliton wave depended on the propagation distance by studying the effect of slow time, according to this relationship (t_R=L/C). Thus, we made it clear that the soliton wave depended on the propagation distance and the chirp parameter C. The characteristics that were used in the SiN microresonator in the anomalous dispersion regime were given in Table (1).

This microresonator was constructed of silicon nitride, a dielectric material commonly employed in linear and nonlinear optical applications. It possesses an extremely transparent window, minimal intrinsic loss, and a refractive index that allows for modest optical field confinement in waveguides. Nonlinear Kerr coefficients in silicon-rich silicon nitride waveguides made them appealing for nonlinear optics. In this situation, the detuning frequency and the noise strength term are both ignored.

We ran the pulse for various chirp values, C=-1, -2, -3, -4, the same is shown in (fig. 3). While (fig. 2) showed the inputs and outputs of a Gaussian pulse in anomalous

dispersion systems of a Gaussian pulse before we entered the effect of the chirped.

The chirp parameter's value of -1 added to the GVD's negative chirp made the chirp parameter's net value negative. This indicates that the pulse broadens because GVD dominated during the initial phases of propagation. The effect of the initial chirp decreases as shown in (fig. 3).

The pulse's shape or the distribution of intensity over time, was changedparticularly in the chirp at the edges. While the center stays close to the Gaussian wave. As a result, we can observe that the outgoing pulse, which was initially a Gaussian pulse with a small value of c, started to expand as the chirp coefficient increased and eventually split at the apex, appearing to be the result of two separate Gaussian pulses combined. From the power spectrum, we noticed that the greater the effect of the chirp factor, the greater the number and intensity of the patterns was shown x), as shown in Figure (4a-4d)). Also, the center frequency almost began to disappear as a result of the growth in the adjacent frequencies to the right and left.
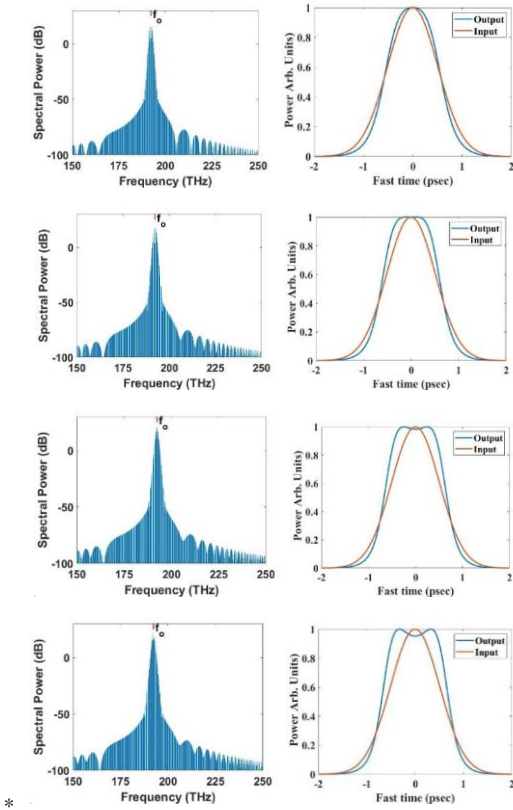

Fig. 2: Input and output of a Gaussian pulse in anomalous dispersion regimes for a Gaussian pulse that is initially unchirped (C=0), and the input power $P_0 = (0.5, 1, 1.5, 2)\ W$.
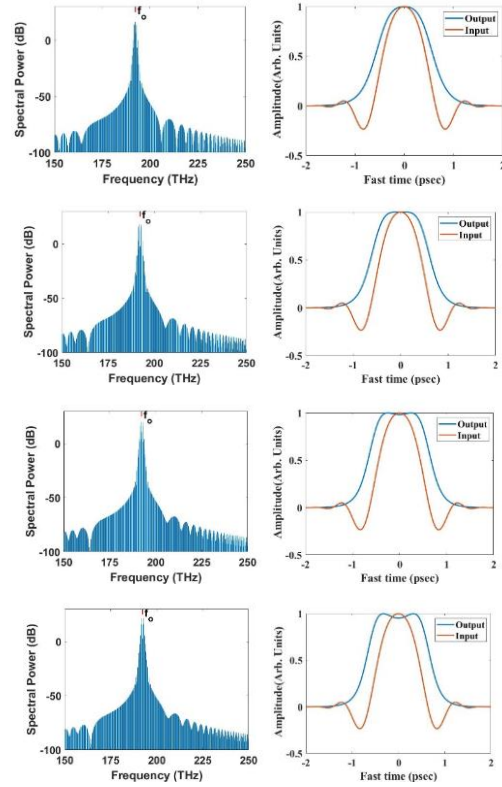

Fig. 3a: describes the propagation of Gaussian pulse in the frequency domain with $P_0 = (0.5, 1, 1.5, 2)W$ respectively and C = -1
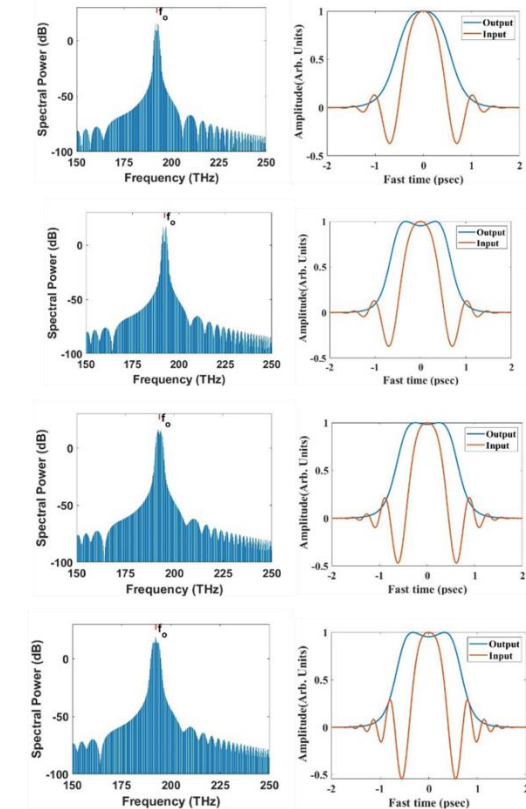

Fig. 3b: describes the propagation of Gaussian pulse in the frequency domain with $P_0 = (0.5, 1, 1.5, 2)$ W respectively and C = -2
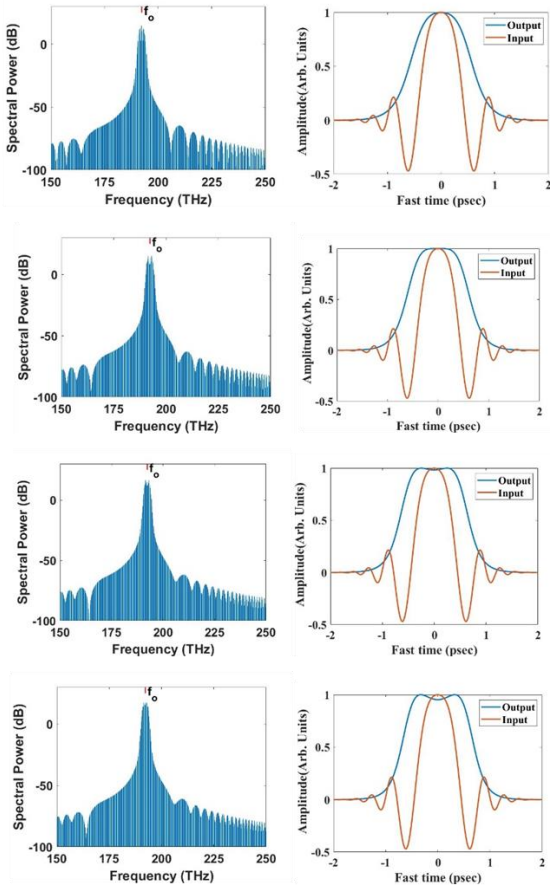
Fig. 3c: describes the propagation of Gaussian pulse in the frequency domain P_0 = (0.5, 1, 1.5, 2) W respectively and C = -3
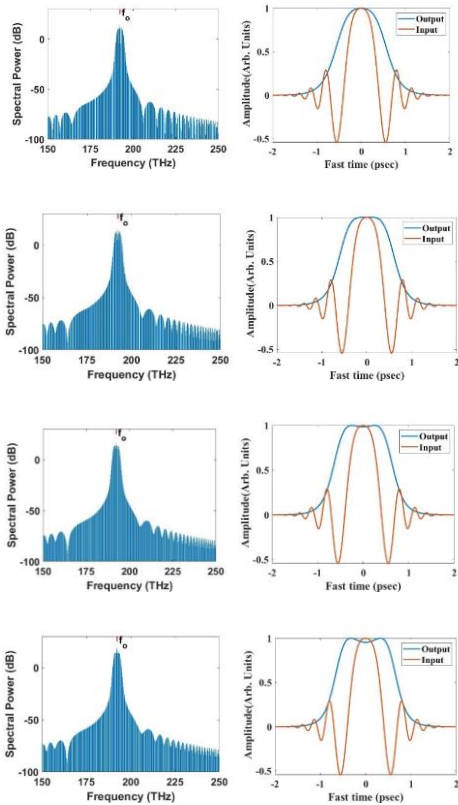

Fig. 3d: describes the propagation of Gaussian pulse in the frequency domain with P_0 = (0.5, 1, 1.5, 2) W respectively and, C = -4

b) Gaussian versus super-Gaussian beams

Group velocity dispersion (GVD) and chirp work together to provide a pulse response that is drastically different from nonlinear effects. Dispersion regions, such as the normal and abnormal regions of dispersion, also influence the action. While the value of β_2 in the normal dispersion region is more than zero. β_2 will be less than zero in the abnormal dispersion region. One can examine the super-Gaussian pulses and their distinctive transmission characteristics for a range of pulse durations and super-elevation properties in both the dispersive and chirp effects domains [31].

The shape of super-Gaussian pulses is comparable to that of a square digital pulse and is considered as one benefit of using them. The Lugatio-Lefever equation was used to examine the results of studying the super-Gaussian pulse dispersion and chirp effects. Because of the complicated nature of the super-Gaussian pulse, this equation is not analytically solvable. As a result, the numerical approaches are employed [32]. The Fourier split stages are the most often used well-known numerical technique for solving it [33].

We used a superwave in our study because we need to explore the use of a super-gaussian pulse and its impact on the microresonator output, particularly in the field of communications. For this purpose, we first developed the concept of a super-Gaussian beam. After solving equation (2) analytically with a MATLAB program and the values of the parameters that were listed in Table (1), we applied the split-step Fourier technique.

We observed from the simulation that the Super-Gaussian pulses, also known as super-gaussian beams, had distribution distribution distribution deviated from the typical Gaussian distribution. They exhibit sharper leading edges and tails compared to Gaussian pulses, and that indicated of having more pronounced variation in intensity from the center to the edges of the pulse.

When super-Gaussian pulses propagated through microresonators, they experienced more significant expansion or spreading compared to Gaussian pulses. This expansion occurred due to the higher frequency components present in the sharper edges of super-Gaussian pulses. As the pulse propagated, these higher frequency components spread out, leading to have broadening pulse shape.

Figure (4) and Figure (5a-5c) depicted the comparison of super-Gaussian pulse propagation along the microresonator with different values of the parameter "m." The "m" value determines the shape of the super-Gaussian pulse, with higher values resulting in sharper edges and tails.

Moreover, we observed from Fig.(5a-5c) an increasing in the power of the input pulse, and that caused the ultra-Gaussian pulse to become shorter. This phenomenon occurred because of the higher input power which leads to have stronger nonlinear effects in the propagation medium. These nonlinear effects can cause self-phase modulation,

which altered e the pulse's phase and amplitude. Consequently, the pulse shape can be compressed, resulting in a shorter duration.
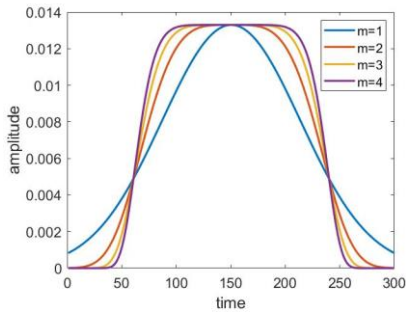

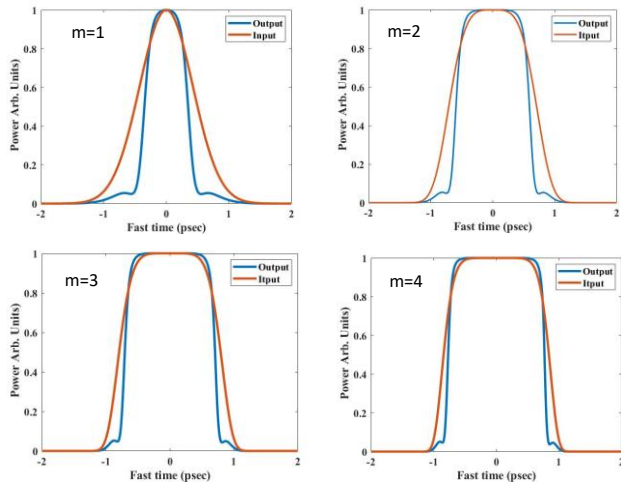Fig. 4: The effect of various m values on the super- Gaussian pulse along the microresonator

Fig. 5a: describes the propagation of super-Gaussian pulse in the frequency domain with P_0 =0.5 for m = 1, 2, 3, 4 respectively.
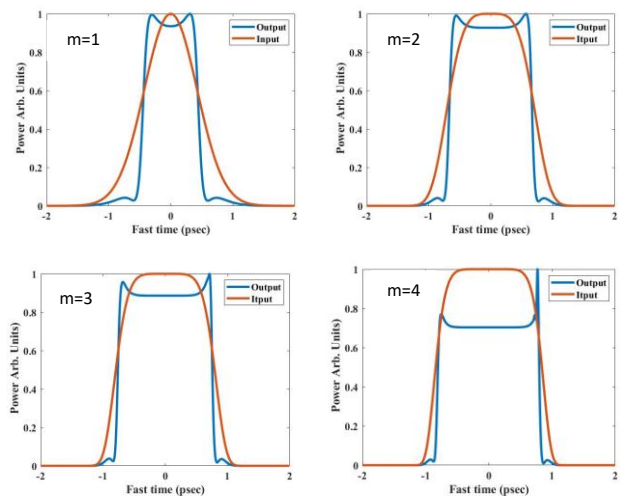

Fig. 5b: describes the propagation of super-Gaussian pulse in the frequency domain with P_0 =1 for m = 1, 2, 3, 4 respectively.
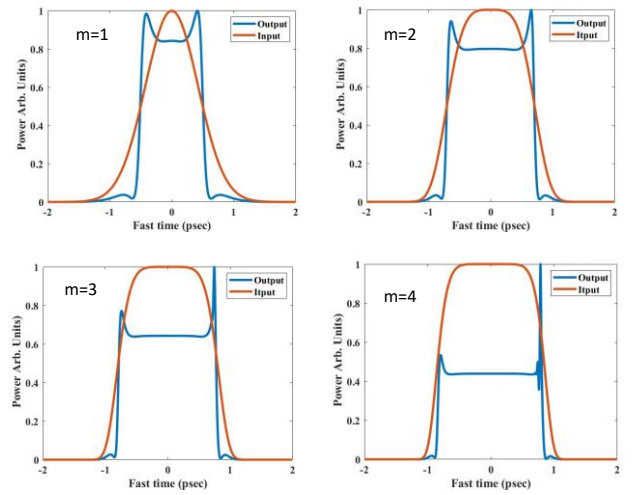

Fig. 5c: describes the propagation of super-Gaussian pulse in the frequency domain with P_0 =1.5 for m = 1, 2, 3, 4 respectively.

At a power value of 1W or more, we noticed a higher super factor, and more dispersion in the outgoing pulse. It looked like it was composed of two Gaussian pulses with pulses with the right side dominating due to dispersion. The power spectrum also expanded at frequencies to the left and right of the center frequency, f_0, but asymmetrically, from the secondary frequencies and the major frequencies (to the right and left of the center frequency).

IV. CONCLUSIONS

We solved the lugatio-Lefever equation (LLE) using the split-step Fourier technique (SSFM) in simulations to show the impact of the input pulses on soliton formation and the optical frequency comb (OFC). We also showed how chirped, super-Gaussian, and Gaussian pulses affected the soliton and OFC. Our study established the pulse link between the input and output, which showed that the soliton and OFC generation features depend on the input pulse for various OFC scenarios.

CONFLICT OF INTEREST

Authors declare that they have no conflict of interest.

REFERENCES

[1] O. Descalzi, Clerc M., Residori S. & Assanto, G. Localized States in Physics: Solitons and Patterns, *Springer-Verlag Berlin Heidelberg*, 2011.

[2] H.G. Purwins, H.U. Bodeker, and S. Amiranashvili, "Dissipative solitons," *Advances in Physics*, Volume 59, Issue 5, 2010.

[3] T. J. Kippenberg, A. L. Gaeta, M. Lipson, and M. L. Gorodetsky, "Dissipative Kerr solitons in optical microresonators," *Science* 361, eaan8083, 2018.

[4] T. Herr, V. Brasch, J. D. Jost, C. Y. Wang, N. M. Kondratiev, M. L. Gorodetsky, and T. J. Kippenberg, "Temporal solitons in optical microresonators," *Nat. Photonics* 8, 145–152, 2014.

[5] M. Yu, J. K. Jang, Y. Okawachi, A. G. Griffith, K. Luke, S. A. Miller, X. Ji, M. Lipson, and A. L. Gaeta,

"Breather soliton dynamics in microresonators," *Nature Communications* 8, 14569, 2017.

[6] Z. S. Abdul-Hussain and H. A. Sultan, A theoretical study of soliton in photonic crystal fibers, *Researcher*, 11(1), 2019.

[7] S. Maatoq and H. A. Sultan, Optical frequency comb generation in semiconductor lasers using optical injection locking technique, *Journal of Basrah Researches ((Sciences))* Vol. (47). No. 1, 2021.

[8] M. S. Jasima, H. A. Sultan, and C. A. Emshary, The effect of attenuation and dispersion on the propagation of a short Gaussian pulse in optical fibers, *Researcher*, 11(1), 2019.

[9] M. S. Jasima, H. A. Sultan and C. A. Emshary, "Study the Effect of Some Photonic Crystal Arrangements on the Dispersion and Effective Refractive Index of Photonic Crystal Fiber", *International Journal of Science and Research (IJSR)*, 2018.

[10] A. Anashkina, P. Marisova, A. Sorokin and V. Andrianov, "Numerical Simulation of Mid-Infrared Optical Frequency Comb Generation in Chalcogenide As_2S_3 Microbubble Resonators", *Photonics*, 6, 55, 2019.

[11] M. Karpov, M. H. P. Pfeiffer, H. Guo, W. Weng, J. Liu, and T. J. Kippenberg, "Dynamics of soliton crystals in optical microresonators," *Nat. Phys.* 15, 1071–1077, 2019.

[12] Q.-F. Yang, X. Yi, K. Y. Yang, and K. Vahala, "Stokes solitons in optical microcavities," *Nat. Phys.* 13, 53–57, 2017.

[13] A. W. Bruch, X. Liu, Z. Gong, J. B. Surya, M. Li, C.-L. Zou, and H. X. Tang, "Pockels soliton microcomb," *Nat. Photonics* 15, 21–27, 2021.

[14] H. Bao, A. Cooper, M. Rowley, L. Di Lauro, J. S. Totero Gongora, S. T. Chu, B. E. Little, G.-L. Oppo, R. Morandotti, D. J. Moss, B. Wetzel, M. Peccianti, and A. Pasquazi, "Laser cavity-soliton microcombs," *Nat. Photonics* 13, 384–389, 2019.

[15] E. Nazemosadat, A. Fulop, O. B. Helgason, P.-H. Wang, Y. Xuan, D. E. Leaird, M. Qi, E. Silvestre, A. M. Weiner, and V. Torres-Company, "Switching dynamics of dark-pulse Kerr frequency comb states in optical microresonators," *Phys. Rev. A* 103, 013513, 2021.

[16] A. B. Matsko, A. A. Savchenkov, W. Liang, V. S. Ilchenko, D. Seidel, and L. Maleki, Mode-locked Kerr frequency combs, *Opt. Lett.* 36, 2845-2847, 2011.

[17] S. Coen, H. G. Randle, T. Sylvestre, and M. Erkintalo, "Modeling of octave-spanning Kerr frequency combs using a generalized mean-field Lugiato-Lefever model", *Opt. Lett.* 38, 37-39, 2013.

[18] Xue X, Xuan Y, Liu Y, Wang PH, Chen S, Wang J, ELeaird D, Qi M, Weiner A, "Mode-locked dark pulse Kerr combs in normal-dispersion microresonators". *Nature Photonics* 9:594–600. 10.1038.137, 2015.

[19] Kilian Seibold, Riccardo Rota, Fabrizio Minganti, and Vincenzo Savona, "Quantum dynamics of Dissipative Kerr solitons", *Quantum Physics*, Dec 2021.

[20] Agrawal, G. Nonlinear Fiber Optics, Academic, San Diego, 2006.

[21] T. Hansson, S. Wabnitz, "Frequency comb generation beyond the Lugiato–Lefever equation: multi-stability and super cavity solitons". *Journal of the Optical Society of America B* 32(7):1259–1266, 10.1364/JOSAB.32.001259, 2015.

[22] X. Xue, Y. Xuan, Y. Liu, PH Wang, S. Chen, J. Wang, D. ELeaird, M. Qi, A.Weiner, "Mode-locked dark pulse Kerr combs in normal-dispersion microresonators". *Nature Photonics* 9:594–600. 10.1038, 137, 2015.

[23] G. Moille, Q. Li, S. Kim, D. Westly, K. Srinivasan, "Phased-locked two-color single soliton microcombs in dispersion-engineered Si3N4 resonators". *Optics Letters* 43(12):2772–2775. 10.1364/OL.43.002772, 2018.

[24] V. Brasch, M. Geiselmann, T. Herr, G. Lihachev, M. H. P. Pfeiffer, M. L. Gorodetsky and T. J. Kippenberg, "Photonic chip-based optical frequency comb using soliton Cherenkov radiation", *Science* 351, 357, 2016.

[25] X. Ji, F. A. S. Barbosa, S. P. Roberts, A. Dutt, J. Cardenas, Y. Okawachi, A. Bryant, A. L. Gaeta and M. Lipson, "Ultra-low-loss on-chip resonators with sub-milliwatt parametric oscillation threshold", *Optica* 4, 619, 2017.

[26] M. Justin, M. Boudoue Hubert, G. Betchewe, Doka, Serge Yamigno, K. Timoleon Crepin, "Chirped solitons in derivative nonlinear Schrodinger equation", *ELSEVIER*, Volume 107, Pages 49-54, February 2018.

[27] N. Aziz, Aly R. Seadawy, U. Raza, K. Ali and Syed T. R. Rizvi, "chirped optical pulses for generalized longitudinal Lugiato Lefever: cubic nonlinear Schrodinger equation", Sprenger, 24 August 2022.

[28] Haus, H. A., Fujimoto, J. G. & Ippen, E. P. "Structures for additive pulse mode locking", *J. Opt. Soc. Am. B* Vol. 8(No. 10): 2068–2076, 1991.

[29] Senior, J. M., & Jamro, M. Y. "Optical fiber communications: principles and practice". *Pearson Education*. 2009.

[30] Agrawal, G. nonlinear Fiber Optics. 5th ed (Amsterdam: Academic), 2012.

[31] T. Murakawa and T. Konishi, "Pulse-by-pulse near 800-nm band power stabilization using all-optical limiter based on self-phase modulation". *Optics Communications*, 344, 134-138. 2015.

[32] M. Teucher and E. Bordignon, "Improved signal fidelity in 4-pulse DEER with Gaussian pulses". *Journal of Magnetic Resonance*, 296, 103-111. 2018.

[33] A. M. Ayela, G. Edah, C. Elloh, A. Biswas, M. Ekici, A. K. Alzahrani, and M. R. Belic, "Chirped super–Gaussian and super–sech pulse perturbation of nonlinear Schrodinger's equation with quadratic–cubic nonlinearity by variational principle". *Physics Letters A*, 396, 127231. 2021.